Energy and angular differential probabilities for photoionization of He using chirped attosecond soft-x-ray pulses

Teck-Ghee Lee, M. S. Pindzola, and F. Robicheaux
Department of Physics, Auburn University, Auburn, Alabama 36849, USA
(Received 7 January 2009; published 29 May 2009)

Based on the time-dependent close-coupling method, energy and angular differential probabilities for various ionization processes of He atoms subjected to intense attosecond soft-x-ray pulses with a photon energy of 91.6 eV and a peak intensity of 10^{15} W/cm^2 are calculated to explore their dependence on the duration and the chirp of the pulse. It is found that the single and the double electron energy distributions for two-photon double ionization are rather sensitive to chirps. That is, both the magnitudes and locations of the sequential peaks in the single electron energy distributions vary strongly with chirps and the two-electron energy distributions being broadened and stretched along the equal energy sharing direction as opposed to the usual total excess energy direction for the case of zero chirp. In addition, our calculation also reveals an unexpected structure formed between the two sequential peaks. In order to better understand the chirp effects on both independent-electron and correlated electron emissions and their relations to the origin of the structure, we analyzed the corresponding probability differential in energy and angle.

DOI: 10.1103/PhysRevA.79.053420 PACS number(s): 32.80.Rm, 32.80.Fb, 42.50.Hz

I. INTRODUCTION

Owing to the rapid advances in technology for strong and short laser pulses, atomic and molecular ionization in intense laser fields has received considerable attention in the past few years, both experimentally and theoretically. From the experimental side, the developments of techniques in ultrafast science have allowed the production of laser pulses with reproducible temporal evolution of the electric field by using phase-stabilized optical frequency comb methods [1,2]. Intense and ultrashort x-ray pulses with durations on the order of a few hundred attoseconds, produced by means of the high-order harmonic generation (HHG) technique [3] and that may attain intensities greater than 10^{14} W/cm^2, have broken new ground for the investigations of the ultrafast breakup dynamics of few-electron atomic and molecular systems. For example, extreme ultraviolet (xuv) pulses with photon energy of 27.9 eV and a pulse duration of 950 as have been characterized by an autocorrelation technique [4], and the two-photon double ionization and above threshold ionization of atomic helium induced by the Ti:sapphire 27th harmonic pulse with photon energy of 41.8 eV have been recently observed [5]. There is no doubt that more experimental measurements will be carried out with much higher peak intensities and much shorter pulse durations in the near future.

From the theoretical standpoint, for moderately short pulses, various state-of-the-art approaches, based on the solution of time-dependent Schrödinger equation (TDSE), have been developed and improved in order to study the response of the ejected electrons to temporal laser pulses. Among the successful ones are the direct numerical integration of the two-electron TDSE with a finite-difference-basis set scheme on a lattice [6], the time-independent *R*-matrix Floquet theory for the two-photon double ionization process of He [7], the two-electron time-dependent close-coupling (TDCC) method [8–10], a mixed atomic *B*-spline spectral and configuration interaction method [11,12], the Jacobi matrix with spectral approach [13,14], and the TDSE with correlated multichannel states [15,16], to name just a few. One of the aims of these theories is to gain a better understanding of electron-electron correlation, in particular, the sequential and nonsequential ionization mechanisms in the two-photon double ionization process of He over a wide range of photon energies.

Photons with energy beyond the complete breakup threshold of 79 eV for He, that is to say a soft-x-ray pulse of 3.2 a.u. or 87 eV photon energy with a laser peak intensity around 10^{16} W/cm^2, have been considered in the pioneering TDSE lattice work of Parker *et al.* [6]. Recently, from the direct solutions of TDSE, Ishikawa and Midorikawa [17] predicted that an anomalous component is present between the two peaks in the electron energy spectra for two-photon double ionization of He by 450, 225, and 150 as soft-x-ray pulses with photon energy of 91.45 eV at peak field intensity of 10^{15} W/cm^2. With the aid of a semiclassical stochastic model, they discussed the origin of the anomalous component and attributed it to a derivative of sequential ionization, namely, due to the postionization energy exchange and second ionization during the core relaxation. Slightly later, a more detailed analysis based on polar plots of the angular distributions of the ejected electrons, the basis set expansion method of Barna *et al.* [18], concluded that the anomalous component actually arises from the electron correlation induced ionization, whereas the two peaks referred to as sequential ionization [17] or as above threshold double ionization [6] are from independent particle ionization that has little to do with electron correlation effects.

While there exist many theoretical studies for two-photon double ionization, the chirp effects on the ejected electrons have not been examined even though chirped pulses play a crucial role in laser technology and chirp is inherent in the attosecond generation process except near the cutoff frequency [3]. In the present work, we attempt to understand how the ejected electron distribution varies as a function of chirp parameters. Specifically, by directly solving the TDSE

in a laser field, we carry out extensive TDCC calculations to investigate not only the single and double electron energy distributions but also the probability differential in energy and angle for two-photon double ionization of He(^1S) subjected to a chirped 450 as x-ray pulses with a photon energy of 91.6 eV and a laser peak intensity of 10^{15} W/cm^2 (corresponding to experimental high-intensity laser pulses with 13.5 nm wavelength [19] which are the 59th harmonic of a 800 nm wavelength Ti:sapphire laser). Some laser-pulse parameters chosen here are essentially the same as in Refs. [17,18] with a purpose to compare the present unchirped results with the earlier calculations to illustrate the numerical accuracy of our calculations. For two-photon absorption, the total angular momentum of the two photoelectrons is a sum of $L=0$ and $L=2$ waves.

This paper is organized as follows. In Sec. II, we briefly recapitulate the TDCC theoretical approach. In Sec. III, we present and discuss the single and the double electron energy distributions and the corresponding probability differential in energy and angle for the chirped and the transform-limited pulses. Section IV summarizes our investigation. Atomic units ($m_e=\hbar=e=1$) are used throughout the paper unless otherwise stated.

II. THEORY

The time-dependent Schrödinger equation for helium in a strong linearly polarized electromagnetic field is given by

$$i\frac{\partial\Psi(\vec{r}_1,\vec{r}_2,t)}{\partial t}=(H_{atom}+H_{rad})\Psi(\vec{r}_1,\vec{r}_2,t), \tag{1}$$

where

$$H_{atom}=-\frac{1}{2}\nabla_1^2-\frac{1}{2}\nabla_2^2-\frac{Z}{r_1}-\frac{Z}{r_2}+\frac{1}{|\vec{r}_1-\vec{r}_2|}, \tag{2}$$

$$\begin{aligned}H_{rad}=&E_0\exp[-2\ln(2)(t-2T)^2/T^2]\\&\times[r_1\cos(\theta_1)+r_2\cos(\theta_2)]\cos\{\omega(t-2T)\\&+[4\ln(2)\eta](t-2T)^2/(2T^2)\},\end{aligned} \tag{3}$$

where $Z=2$ is the atomic number, E_0 is the electric field strength, T is the full width at half maximum (FWHM) pulse length, ω is the radiation field frequency, and η stands for the dimensionless chirp parameter. The positive or negative values of η represent the instantaneous laser frequency increases or decreases with time. It can be shown that the duration (FWHM) of the chirped pulse, T_{FWHM}, is related to the duration of the transform-limited pulse by $T_{\mathrm{FWHM}}=T\sqrt{1+\eta^2}$. For the xuv pulse described with Eq. (3), with nonzero chirp parameters, the laser frequency bandwidth is given by $\Delta\omega=4\ln(2)\sqrt{1+\eta^2}/T$.

The total wave function is expanded in coupled spherical harmonics for each total orbital and spin angular momentum, LS,

$$\Psi^{LS}(\vec{r}_1,\vec{r}_2,t)=\sum_{l_1,l_2}\frac{P^{LS}_{l_1l_2}(r_1,r_2,t)}{r_1r_2}\sum_{m_1,m_2}C^{l_1l_2L}_{m_1m_20}Y_{l_1m_1}(\hat{r}_1)Y_{l_2m_2}(\hat{r}_2). \tag{4}$$

Upon substitution of the total wave function into the time-dependent Schrödinger equation, we obtain the following set of time-dependent close-coupled partial differential equations [10]:

$$\begin{aligned}i\frac{\partial P^{LS}_{l_1l_2}(r_1,r_2,t)}{\partial t}=&T_{l_1l_2}(r_1,r_2)P^{LS}_{l_1l_2}(r_1,r_2,t)\\&+\sum_{l_1',l_2'}V^{L}_{l_1l_2,l_1'l_2'}(r_1,r_2)P^{LS}_{l_1'l_2'}(r_1,r_2,t)\\&+\sum_{L'}\sum_{l_1',l_2'}W^{LL'}_{l_1l_2,l_1'l_2'}(r_1,r_2,t)P^{L'S}_{l_1'l_2'}(r_1,r_2,t),\end{aligned} \tag{5}$$

where the kinetic and nuclear energy operator is $T_{l_1l_2}$, the electron-electron interaction energy operator is $V^{L}_{l_1l_2,l_1'l_2'}$, and the time-dependent radiation field operator is $W^{LL'}_{l_1l_2,l_1'l_2'}$. The time-dependent close-coupled equations are solved using a discrete representation of the radial wave functions and all operators on a two-dimensional lattice.

The initial condition for the radial wave functions of Eq. (5) is given by

$$P^{LS}_{l_1l_2}(r_1,r_2,t=0)=\bar{P}_{ll}(r_1,r_2)\,\delta_{L,0}\delta_{S,0}\delta_{l_1,l}\delta_{l_2,l}, \tag{6}$$

where the radial wave functions $\bar{P}_{ll}$ are obtained by solution of a set of time-dependent close-coupled partial differential equations for the imaginary time relaxation of Eq. (1) with $H_{rad}=0$. After propagation of the time-dependent close-coupled equations, momentum space wave functions at final time t_f are extracted through

$$\begin{aligned}P^{LS}_{l_1l_2}(k_1,k_2)=&\int_0^\infty dr_1\int_0^\infty dr_2P_{k_1l_1}(r_1)P_{k_2l_2}(r_2)\\&\times[P^{LS}_{l_1l_2}(r_1,r_2,t=t_f)-\mathcal{L}P^{LS}_{l_1l_2}(r_1,r_2,t=0)],\end{aligned} \tag{7}$$

where

$$\mathcal{L}=\int_0^\infty dr_1\int_0^\infty dr_2P^{LS}_{l_1l_2}(r_1,r_2,t=0)P^{LS}_{l_1l_2}(r_1,r_2,t=t_f) \tag{8}$$

and $P_{kl}(r)$ are He^+ continuum radial wave functions.

Various probability functions are used to analyze the effect of a strong electromagnetic field on the helium atom. A double energy probability function is given by

$$\frac{d^2\mathcal{P}}{dE_1dE_2}=\frac{1}{k_1k_2}\sum_{LS}\sum_{l_1,l_2}|P^{LS}_{l_1l_2}(k_1,k_2)|^2, \tag{9}$$

a single energy probability function is given by

$$\frac{d\mathcal{P}}{dE_1} = \frac{1}{k_1}\int_0^\infty dk_2 \sum_{LS}\sum_{l_1,l_2} |P^{LS}_{l_1 l_2}(k_1,k_2)|^2, \tag{10}$$

and the total probability for photoionization is given by

$$\mathcal{P} = \int_0^\infty dk_1 \int_0^\infty dk_2 \sum_{LS}\sum_{l_1,l_2} |P^{LS}_{l_1 l_2}(k_1,k_2)|^2. \tag{11}$$

For a detailed analysis of two-electron correlation effects, one may define a triple differential probability function in both energy and angle given by

$$\frac{d^3\mathcal{P}}{dE_1 d\Omega_1 d\Omega_2} = \frac{1}{k_1}\int_0^\infty dk_2 \left| \sum_{LS}\sum_{l_1,l_2} (-i)^{l_1+l_2} e^{i(\sigma_{l_1}+\sigma_{l_2})} P^{LS}_{l_1 l_2}(k_1,k_2) \times \sum_{m_1,m_2} C^{l_1 l_2 L}_{m_1 m_2 0} Y_{l_1 m_1}(\hat{k}_1) Y_{l_2 m_2}(\hat{k}_2) \right|^2, \tag{12}$$

where σ_l is a Coulomb phase shift.

III. RESULTS AND DISCUSSION

In this investigation, we consider a He atom exposed to a linearly polarized attosecond xuv pulse with a Gaussian envelope expressed in Eq. (3). The central frequency ω of the laser pulse corresponds to the 59th harmonic of a Ti:sapphire laser with photon energy of 91.6 eV. The pulse durations (FWHM) of interest here are 135 and 450 as which correspond to $T=5.58$ and 18.6 a.u., respectively. The period of the pulse cycle is given by $T_c=2\pi/\omega=1.87$ a.u. The laser-pulse peak intensity is 10^{15} W/cm^2. The close-coupled equations with the radiation field are then solved on a uniform numerical lattice using standard finite-difference schemes. About 500 imaginary time steps at $\Delta\tau=0.01$ a.u. are used for relaxation to reach convergence on a mesh with step size of $\Delta r_1=\Delta r_2=0.1$ a.u. With these step sizes, the ground state of helium has a total energy of −78.1 eV on the lattice compared to the exact value of ionization potential energy $I_p=-79$ eV. For the 450 as pulse, we have employed 2360×2360 grid points so that the maximum radial box size is $R=236$ a.u. Starting from the ^1S of He at $t=0$, the wave function subjected to the laser pulse is propagated to roughly $t_f=5.5T$ with a temporal step size of 0.001 a.u. to ensure the convergence of the triple differential probabilities. For the 135 as pulse, we found that a smaller box size of $R=160$ a.u. is adequate but longer time propagation is necessary (e.g., up to $10T$) in order to achieve reasonable convergence especially for the case when the two electrons share the same excess energy (see below). The partial waves considered here which are $0\le l_1$, $l_2\le 3$ that coupled to total angular momenta $L\le 2$ are sufficient for the present investigation. Additional convergence checks, carried out with a bigger box size (e.g., 288 a.u.) and smaller integration step sizes, have led to virtually identical results.

A. Electron energy spectra

A schematic representation of helium energy levels involved in the double ionization by absorption of two photons for a photon energy of 91.6 eV or 3.37 a.u. with a 10^{15} W/cm^2 peak laser intensity is shown in Fig. 1. For two-photon double ionization by xuv pulses with $\omega=91.6$ eV which is much greater than the 54.4 eV binding energy of He$^+$ ions, both sequential and nonsequential channels are open. In the nonsequential or direct process, two electrons share the total excess energy, which give rise to a relatively uniform electron energy distribution, while the sequential process leads to an energy distribution that displays two pronounced peaks of energies, $E_1=\omega-24.6$ eV and $E_2=\omega-54.4$ eV, resulting from ejecting electron out of He and He$^+$.

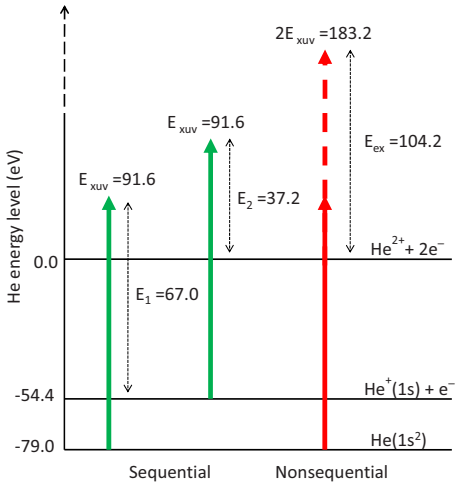

FIG. 1. (Color online) A schematic diagram of the He energy levels involves in two-photon double ionization process.

Results from the absorption of two photons by the electron pair at the end of various pulses are shown in Fig. 2. The single electron energy distributions integrated over the second electron given by Eq. (10) for a pulse duration of 450 as shown in Fig. 2(a), in which the two photons are predominantly absorbed one after the other almost independently of each other, can be clearly identified as two prominent peaks of energies E_1 and E_2, resulting from the ionization of He and He$^+$ [18]. These peaks are separated by an energy gap of roughly $E_1-E_2=30$ eV. The origin of this energy gap is known and is from the difference between the fully correlated ground state energy of 79 eV and total energy of a two independent-electron model (i.e., 49 eV) of the He atom [20]. At a pulse duration of 450 as, the single electron energy spectrum between this energy gap is at a minimum since electron-electron correlation effects are rather small. Furthermore, we notice the formation of two small subpeaks which can be seen at 26.3 and 78 eV. These peaks clearly reflect an excitation process that after the first electron ejection, the second electron is left in the resulting He$^+(n=2)$ states which corresponds to energies at 65.4 eV [i.e., 40.8 eV above the He$^+(1s)$ threshold] and 13.6 eV below the second ionization threshold of 79 eV. Structures from higher excitation levels, i.e., $n\ge 3$, are within the plot but are negligibly small to be visible. These findings are consistent with recent calculations of Ishikawa and Midorikawa [17]. Likewise, similar effects have been noted in more recent studies [18,20].

Together with the transform-limited pulse, in Fig. 2(a), we also present the single electron energy distributions for 450

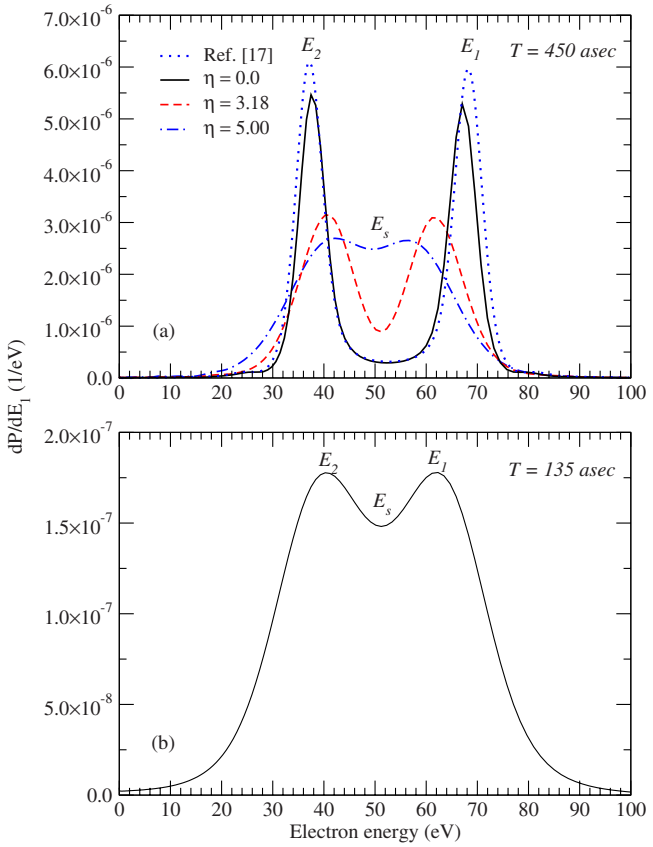

FIG. 2. (Color online) Single electron energy distribution (dP/dE) as a function of ejected electron energy. (a) $T=450$ as pulse. Solid: zero chirp, dashed: chirped with $\eta=3.18$, dotted-dashed: chirped with $\eta=5.00$, and dotted line: calculation from Ref. [17] and (b) $T=135$ as pulse.

as pulses that are chirped. Note that the chirp parameters are chosen arbitrarily except for $\eta=3.18$ which is set to have the same laser frequency bandwidth as the transform-limited 135 as pulse. Interestingly, as the chirp strength increases, Fig. 2(a) shows not only the widths of the E_1 and E_2 peaks being broadened and the maxima being lowered $(\sim 40\%)$ in comparison with the results of the unchirped pulses but the peaks also being shifted toward each other, resulting a smaller energy separation. That is, the energy separations for $\eta=3.18$ and 5.00 are 22 and 16 eV, respectively. The narrowing of the energy separation as the chirp strength increases can be easily understood from the sequential photoabsorption of the He atom. In this situation, the first photon being absorbed by He is at a lower frequency of the oscillating electric field and the second photon being subsequently absorbed by the He^+ ion is at a higher frequency. Although they are not shown here, we have checked this effect by considering the negative chirps (e.g., $\eta=-1.25$ and -3.18) and confirmed they do indeed give the opposite results by widening the energy gap between the two sequential peaks.

Apart from the widths' broadening, the reduction in the peaks' heights, and the energy gaps' narrowing, it appears the "valley" in between the peaks, which describes the electron correlation induced ionization, is being filled and raised dramatically. These effects seem to resemble the outcomes of the use of very short pulses. To gain some insights into such consequences, we plotted the single electron energy distribution for a pulse duration of 135 as in Fig. 2(b) for comparison. Figure 2(b) exhibits two pronounced peaks that situated at $E_1=62$ eV and $E_2=40$ eV. These peaks broaden and move closer toward each other with the valley being raised. This effect has been investigated in a recent study of two-photon double ionization of He but with lower photon energy of $\omega=2.1$ a.u. It is shown that when the pulse becomes very short one sees only a single broad peak. This is because the two-electron single continuum wave packet arises from first photoabsorption process is very localized and electron correlation is very strong, and the wave packet has no time to spread before second photoionization occurs [21]. Comparing the spectrum from the transform-limited $T=135$ as pulse to the long chirped pulses depicted in Fig. 2(a), the rising of the valley for the chirped pulses seems to suggest a possibility that the chirp may stimulate the electron correlation induced ionization. Note that the magnitude difference in the single electron energy spectra for the long and the short pulses is owing to the difference in the total laser power between them.

Were the rising of the valley simply the consequence of the enhancement of the electron correlation induced ionization, the electron energy distribution should closely resemble those of the shorter pulse. So we examine the contour plots of the probability density distribution given by Eq. (9) of energy E_1, E_2 of the two electrons, as shown in Fig. 3. Figure 3(a) shows our reproduction of the result calculated by Ishikawa and Midorikawa (e.g., see Fig. 1(a) in Ref. [17]) for the transform-limited pulse $T=450$ as. Next, we focus on the influence of the chirp on the two-photon double ionization probability density distribution. In the case of single-photon above threshold ionization, the use of chirped pulses with the same intensities and frequency bandwidths as transform-limited pulses does not change the ionized electron energy spectra. But here, for the two-photon double ionization, as we compare Figs. 3(b) and 3(c), we see a contrasting result in the two-electron energy distributions between the chirped and the unchirped pulses; namely, the energy spectra for the chirped pulse are significantly altered. Qualitatively, it seems the nonsequential component has been significantly suppressed by the chirp. Note that the spectral profile of the chirped 450 as pulse with $\eta=3.18$ is essentially identical to that of the transform-limited 135 as pulse (i.e., $\Delta\omega=0.50$).

Figure 4 traces the variation in the probability density distribution for the 450 as pulse as a function of chirp strength. Notice two distinct features here: (i) the effect of chirp has clearly modified the sequential and nonsequential electron distributions and (ii) as the chirp is increased from $\eta=1.25$ to 5.0, we see these distributions being significantly broadened and stretched along the equal energy sharing $E_1=E_2$ axis. In addition, an unexpected structural formation is clearly emerging between the two sequential islands. Could this means that because of the paradigm change in the two-electron energy spectra the structure is induced by some sort of "interference effect" between the nonsequential and sequential processes? At this point, we could not offer any reasonable explanation but an interference as a conjecture for the origin of this structure. Perhaps, by looking at the ejected

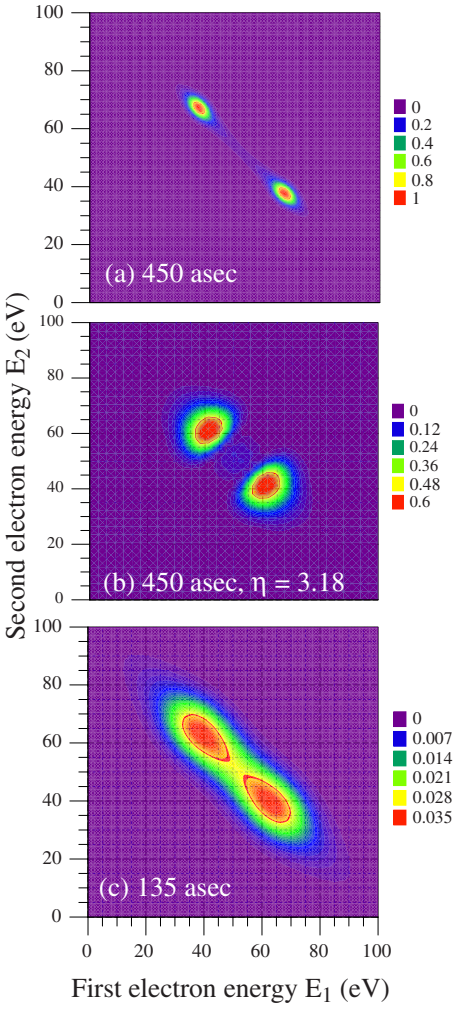

FIG. 3. (Color online) Contour plots of probability density distribution (in arbitrary units) of the energies E_1, E_2 of the two electrons for a pulse with FWHMs of (a) 450 as, (b) 450 as with chirp $\eta=3.18$, and (c) 135 as. Note that the probability scale is relative to the 450 as transform-limited pulse. Also note that the two "teardrop" shapes enclosed by the lighter shading represent the peaks of the probability density distribution.

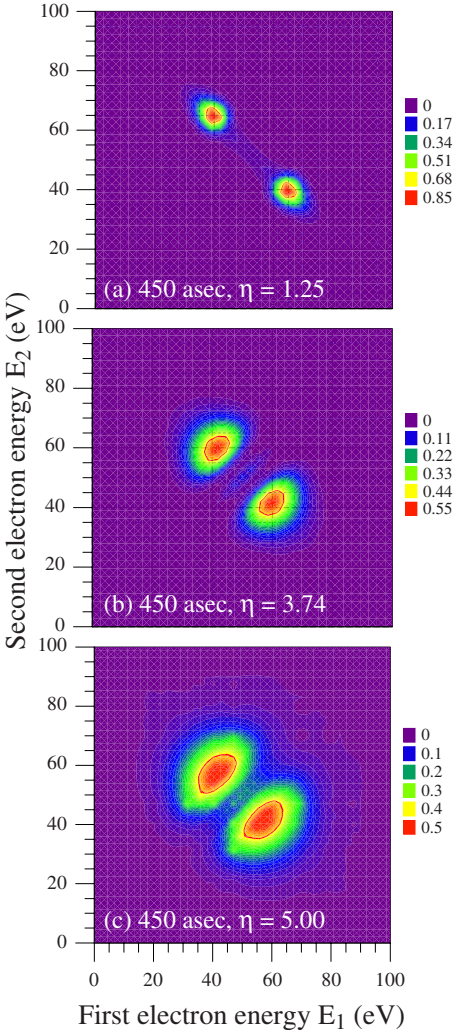

FIG. 4. (Color online) Evolution of the probability density distribution (in arbitrary units) as a function of chirp strength for $T=450$ as pulse. Note that the probability scale is relative to the 450 as transform-limited pulse and the description of the shading representations is the same as in Fig. 3.

electron energy and angular differential probability varies as a function of pulse lengths and chirps in Sec. III B, one could find an answer for the origin of the structure. It is worthwhile to note that the fully integrated electron densities or the total probabilities for photoionization calculated using Eq. (11) for the transform-limited $T=450$ and 135 as pulses are 8.23×10^{-5} and 7.86×10^{-6}, respectively, and for the 450 as chirped pulse with incremental values of $\eta=1.25$, 3.18, 3.74, and 5.00 are found to be 8.28×10^{-5}, 9.29×10^{-5}, 8.93×10^{-5}, and 9.61×10^{-5}, respectively.

B. Energy and angular differential probability

To gain a further understanding of the independent-electron ionization and electron correlation induced ionization with the chirp effects and their relations to the structural formation, we now turn to analyze the energy and angular differential probability. Defining all photoelectron emission angles with respect to the directions of the polarization of the radiation field, triple differential probabilities are presented in Figs. 5–7 as a function ejected electron energies as well as a function of θ_1 and θ_2 for coplanar geometry (i.e., $\phi_1=\phi_2=0°$).

In Fig. 5, we compare the angular differential probabilities at $E_2=37.5$ eV, $E_s=52.3$ eV, and $E_1=67$ eV with $\theta_1=0°$ as shown for transform-limited 450 and 135 as pulses. The probability behaviors for $E_2=37.5$ eV and $E_s=67$ eV are essentially identical for both long and short pulses and are expected since the E_1 and E_2 peaks are symmetrical in both cases. Notice that no matter the laser-pulse length is long or short, the angular differential probabilities at $E_2=37.5$ eV and $E_1=67$ eV exhibit dipolelike pattern, signaling the importance of the independent-electron ionization process [18], even though the probability for the $T=135$ as pulse is roughly 30 times weaker than for the $T=450$ as one. At equal energy sharing of $E_s=52.3$ eV, we see a display of nondipole pattern for ionization probability with strongly

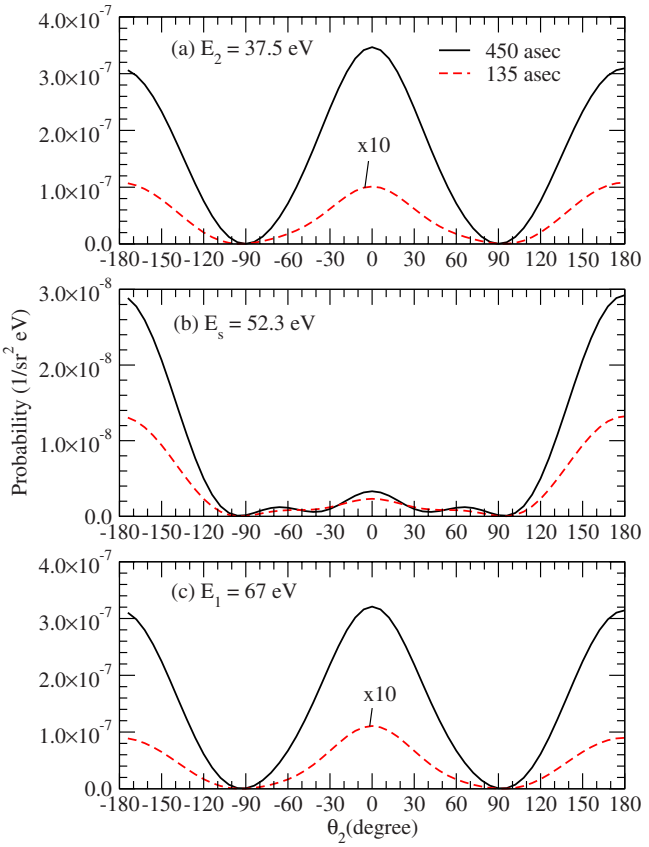

FIG. 5. (Color online) Triple differential probability as a function of ejected electron angle with a specific double-ejection configuration (θ_1=0°) at different energies: 37.5, 52.3, and 67 eV for T=450 and 135 as transfer-limited pulses. Note that except for the E_s=52.3 eV case, the angular differential probabilities for 135 as pulse at E_2=37.5 eV and E_1=67 eV have been multiplied by a factor of 10 for clarity.

suppressed peaks at θ_2=0°. These significantly smaller probabilities correspond to an increase in the correlated emission process. It is worth noticing that the values of the ionization probabilities for both long and short pulses are almost the same especially for the electron-ejected angles between −90° and +90°. Thus, this clearly demonstrates that the dominance of electron correlation for long pulse duration is somehow compatible to the short one. But of course, if one concentrates only on the 135 as pulse and compares the magnitudes of the angular differential probabilities at these electron escaping energies, since their magnitudes are almost equal, one sees an obvious competition between the independent-electron ionization and electron correlation ionization processes. So, one can envisage that when the pulse duration becomes even shorter, the remaining electron in He^+ has no time to relax to a stationary state since the time interval between these two ionization processes becomes too short for the relaxation to happen. In such a situation, the separation between sequential and nonsequential ionizations also becomes unclear. For the long pulse, however, it is obvious that the sequential ionization is the dominant process.

Now let us consider the case when the pulses are chirped as shown in the following figures. In Fig. 6, we present the

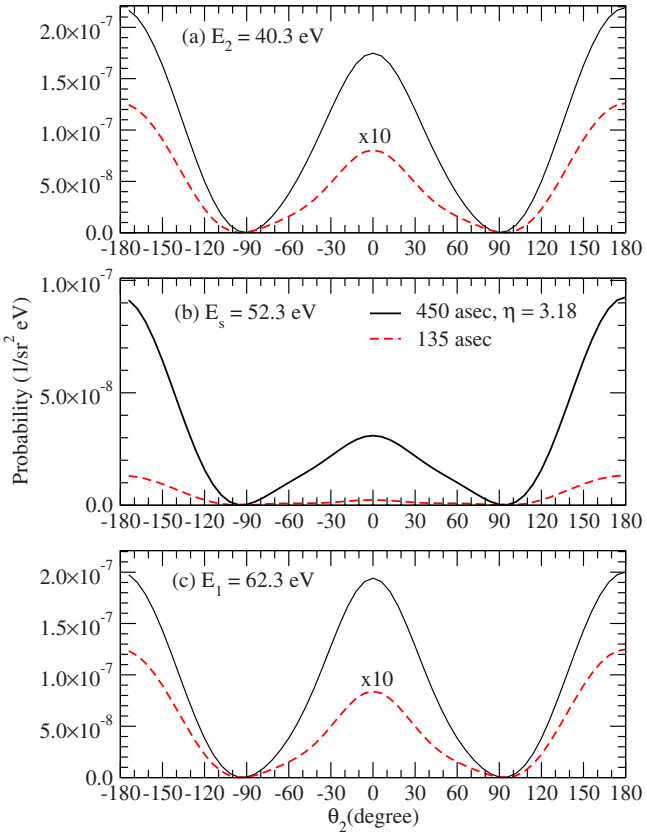

FIG. 6. (Color online) Similar to Fig. 5, but for T=450 as pulse with a chirp of η=3.18 and T=135 as transform-limited pulse.

angular differential probabilities for the T=450 as pulse with a chirp of η=3.18 along with the T=135 as transform-limited pulse at the electron escaping energies of 40.3, 52.3, and 62.3 eV. It is obvious that the angular differential probabilities at their sequential peaks E_2=40.3 eV and E_1=62.3 eV shown in Figs. 6(a) and 6(c) reveal similar trends as displayed in Figs. 5(a) and 5(c) earlier. They remain identically dipole in shape, but their probabilities have been weakened by ~30% in comparison to the unchirped

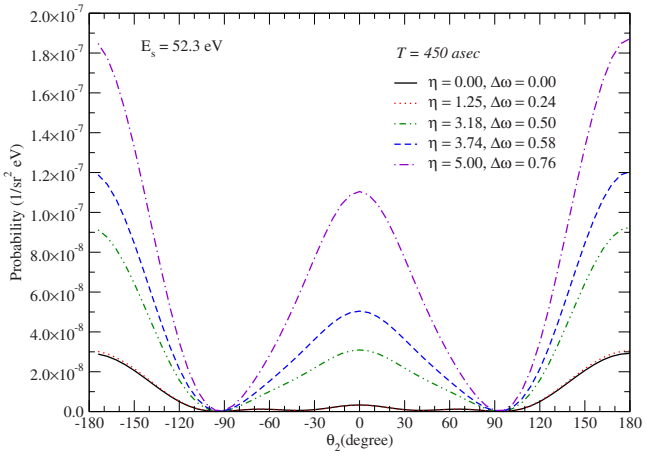

FIG. 7. (Color online) Evolution of the triple differential probability as a function of chirp strength for T=450 as pulse at equal energy sharing E_s=52.3 eV.

$T=450$ as pulse. At equal energy sharing $E_s=52.3$ eV shown in Fig. 6(b), however, the behavior of the probability distribution exhibits a notable transformation from a weak nondipolelike as in cases of unchirped pulses to a strong dipole.

So far, we have learned that the sequential peaks move around with chirps and also illustrated that the angular differential probabilities with their respective E_1 and E_2 peaks decrease as a function of chirp but with their dipole pattern remain intact. We have checked the results for various values of η and confirmed that this is indeed the case. Therefore, in Fig. 7, we shall omit the angular differential probabilities for different sets of E_1 and E_2 but only emphasize on the evolution of the angular differential probabilities for the $T=450$ as pulse as a function of chirp parameter η at equal energy sharing $E_s=53.2$ eV. As the chirp strength is increased, we see that the angular differential probability function changes from nondipole with small probability to dipole with substantially larger probability. This leads us to think that the photoemission process involving electron correlation becomes less probable with chirps. However, this does not tell us whether the transition from a dominant nonsequential to a dominant sequential process is due to either the nonsequential being weakened or the sequential being strengthened or both. In order to have a better idea of how much the nonsequential process varies with chirps, we examine the chirp effects on the double ionization from the P wave, which proceeds through pure nonsequential process, for the unchirped and chirped (e.g., $\eta=5.0$) cases. We find the ionization probability for the zero chirp changes from 2.64×10^{-4} to 2.17×10^{-4} for the chirped pulse, a roughly 20% drops in the probability for the nonsequential process. Now it is clear that there is a transition from a dominant nonsequential ionization to a dominant sequential ionization, and it is this chirp-induced sequential ionization that gives rise to the structure formed between the two peaks in the two-electron energy spectra.

IV. SUMMARY

In this investigation, we have applied the time-dependent close-coupling method to investigate the two-electron emission process from photoionization of He under chirped x-ray pulses with a photon energy of 91.6 eV and an intensity of 10^{15} W/cm^2 generated from the 59th order harmonic of a Ti:sapphire laser. We have shown that our lattice calculation for the single and double electron energy spectra for 450 as pulse with zero chirp agrees well with earlier calculations [17,18]. When the same pulse with different chirps is considered, we have found that, in the single electron energy spectra, the magnitudes and the locations of the sequential peaks depend strongly on the chirps and the valley between the peaks which represent the electron correlation induced ionization also being raised. At first, all these appear to resemble results from the shortening of laser pulses where electron correlation induced ionization becomes prominent. But by carefully analyzing the contour plots of the two-electron ejection probability densities, we realized this is not the case. It is shown that, in contrast to the zero chirp case where the two-electron energy spectra are usually distributed along the total excess energy direction, the chirp effects have caused the change in paradigm by stretching and broadening the two-electron energy spectra along the equal energy sharing axis. Additionally, we have also observed an unexpected structural formation between the two sequential peaks.

To better understand the influences of chirp on the sequential peaks, the nonsequential valley, and the formation of the structure, we have examined the probability differential as a function of electron escaping energies and electron emission angles for the zero chirp and chirped cases. It is found that no matter the pulse is chirped or unchirped, for relatively long pulses, the ionization induced by electron correlation remains weak compared to the independent-electron ionization process. On the other hand, for short transform-limited pulses, we have seen a clear competition between the electron correlation induced ionization and the independent-electron ionization events. Along with these, we have also found the chirp is capable of "simultaneously" modifying the outcomes of the independent-electron ionization and electron correlation induced ionization and is exemplified in the case where two electrons share the total excess energy—an apparent transition from a dominant nonsequential to a dominant sequential ionization as the chirp strength increases. This also brought us to conclude that the origin of the structure formed between the sequential peaks is undoubtedly due to the chirp-induced sequential ionization.

All told, the present results have no available experimental data with which to compare. A possible future experiment that can be carried out is the electron-ion coincidence in which the ejected electron distribution can be mapped out in coincidence with the recoiled He^{2+} ion. Such technique, though an indirect one, will allow one to reveal the evidence of the dynamical electron correlation induced ionization and independent-electron ionization appearing in the electron spectra, as well as the triple differential probabilities for the present chirped and unchirped attosecond pulses.

ACKNOWLEDGMENTS

This work was supported in part by grants from the U.S. National Science Foundation. Computational work was carried out at the National Energy Research Scientific Computing Center in Oakland, California and at the National Center for Computational Sciences in Oak Ridge, Tennessee.

[1] Th. Udem, R. Holzwarth, and T. W. Hansch, Nature (London) **416**, 233 (2002).
[2] A. Baltuska, T. Udem, M. Uiberacker, M. Hentschel, E. Goulielmakis, C. Gohle, R. Holzwarth, V. S. Yakovlev, T. W. H. A. Scrinzi, and F. Krausz, Nature (London) **421**, 611 (2003).
[3] R. Kienberger, E. Gouliemakis, M. Uiberacker, A. Baltuska, V. Yakovlev, F. Bammer, A. Scrinzi, Th. Westerwalbesloch, U. Kleinberg, U. Heinzmann, M. Drescher, and F. Krausz, Nature (London) **427**, 817 (2004).
[4] T. Sekikawa, A. Kosuge, T. Kana, and S. Watanabe, Nature (London) **432**, 605 (2004).
[5] H. Hasegawa, E. J. Takahashi, Y. Nabekawa, K. L. Ishikawa, and K. Midorikawa, Phys. Rev. A **71**, 023407 (2005).
[6] J. S. Parker, L. R. Moore, K. J. Meharg, D. Dundas, and K. T. Taylor, J. Phys. B **34**, L69 (2001).
[7] L. Feng and H. W. van der Hart, J. Phys. B **36**, L1 (2003).
[8] M. S. Pindzola and F. Robicheaux, J. Phys. B **31**, L823 (1998).
[9] J. Colgan and M. S. Pindzola, Phys. Rev. Lett. **88**, 173002 (2002).
[10] M. S. Pindzola, F. Robicheaux, S. D. Loch, J. C. Berengut, T. Topcu, J. Colgan, M. Foster, D. C. Griffin, C. P. Ballance, D. R. Schultz, T. Minami, N. R. Badnell, M. C. Witthoeft, D. R. Plante, D. M. Mitnik, J. A. Ludlow, and U. Kleiman, J. Phys. B **40**, R39 (2007).
[11] S. Laulan and H. Bachau, Phys. Rev. A **68**, 013409 (2003).
[12] S. Laulan and H. Bachau, Phys. Rev. A **69**, 033408 (2004).
[13] E. Foumouo, G. L. Kamta, G. Edah, and B. Piraux, Phys. Rev. A **74**, 063409 (2006).
[14] E. Foumouo, P. Antoine, B. Piraux, L. Malegat, H. Bachau, and R. Shakeshaft, J. Phys. B **41**, 051001 (2008).
[15] L. A. A. Nikolopoulos and P. Lambropoulos, J. Phys. B **40**, 1347 (2007).
[16] P. Lambropoulos and L. A. A. Nikolopoulos, New J. Phys. **10**, 025012 (2008).
[17] K. L. Ishikawa and K. Midorikawa, Phys. Rev. A **72**, 013407 (2005).
[18] I. F. Barna, J. Wang, and J. Burgdörfer, Phys. Rev. A **73**, 023402 (2006).
[19] E. J. Takahashi, Y. Nabekawa, and K. Midorikawa, Appl. Phys. Lett. **84**, 4 (2004).
[20] E. Foumouo, P. Antoine, H. Bachau, and B. Piraux, New J. Phys. **10**, 025017 (2008).
[21] E. Foumouo, S. Laulan, B. Piraux, and H. Bachau, J. Phys. B **39**, S427 (2006).